ACS APPLIED MATERIALS & INTERFACES

Research Article

www.acsami.org

Polyethylenimine-Capped Ag Nanoparticle Film as a Platform for Detecting Charged Dye Molecules by Surface-Enhanced Raman Scattering and Metal-Enhanced Fluorescence

Kwan Kim,*[,†] Ji Won Lee,[†] and Kuan Soo Shin*[,‡]

[†]Department of Chemistry, Seoul National University, Seoul 151-742, Korea

[‡]Department of Chemistry, Soongsil University, Seoul 156-743, Korea

Supporting Information

ABSTRACT: Many drugs are charged molecules and are weak bases or acids having counterions. Their binding to biological surfaces is generally difficult to assess by vibrational spectroscopy. In this work, we demonstrated the potential of surface-enhanced Raman scattering (SERS) conducted using a polyethylenimine (PEI)-capped Ag nanoparticle film for the quantification of an electrostatic adsorption process of charged drug molecules, by using charged dye molecules such as sulforhodamine B (SRB) and rhodamine-123 (R123) as model drugs. It was possible to detect small-sized anions such as SCN^- at 1×10^{-9} M by SERS because of the cationic property of PEI. We were subsequently able to detect a prototype anionic dye molecule, SRB, by SERS at a subnanomolar concentration. On the other hand, it was difficult to detect cationic dyes such as R123 because of the electrostatically repulsive interaction with PEI. Nonetheless, we found that even R123 could be detected at subnanomolar concentrations by SERS by depositing an anionic polyelectrolyte such as poly(sodium 4-styrenesulfonate) (PSS) and poly(acrylic acid) (PAA) onto the PEI-capped Ag nanoparticles. Another noteworthy point is that a subnanomolar detection limit can also be achieved by carefully monitoring the fluorescence background in the measured SERS spectra. This was possible because charged dyes were not in contact with Ag but formed ion pairs with either PEI or PSS (PAA), allowing metal-enhanced fluorescence (MEF). The PEI-capped Ag nanoparticle film can thus serve as a useful indicator to detect charged drug molecules by SERS and MEF.

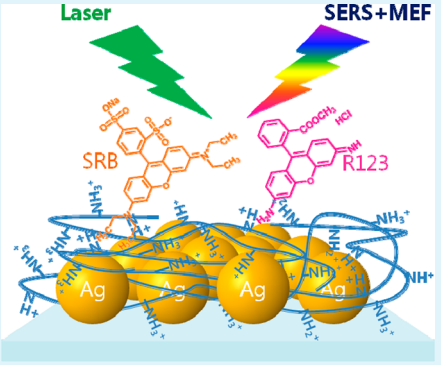

KEYWORDS: *Ag nanoparticles, polyethylenimine, charged dyes, surface-enhanced Raman scattering, metal-enhanced fluorescence*

1. INTRODUCTION

Attraction between unlike charges is a well-established phenomenon even in biological systems.[1,2] Interaction of drug molecules with the cell membrane surface will thus primarily be of an electrostatic character because many drugs are, in fact, charged molecules and are weak bases or acids having counterions.[3−6] However, it is generally difficult to spectroscopically assess how well drug molecules are bound to membrane surfaces because of the low signal levels transmitted.[7,8] In the case of fluorescent drug molecules, membrane binding may be monitored and quantified by fluorescence spectroscopy, but the usual optical and vibrational spectroscopies cannot be used to analyze the amount of drugs bound to membranes.[9−12] One of our ongoing interests is in the development of vibrational spectroscopic methods to highlight the interaction of charged drugs with membranes. Therefore, we aimed to explore the potential of surface-enhanced Raman scattering (SERS) as a powerful tool in quantifying such electrostatic adsorption processes by using charged dyes as model drugs.

SERS is an abnormal surface optical phenomenon that produces strong, increased Raman signals for molecules adsorbed on nanostructured coinage metals.[13,14] Recently, even single-molecule detection by surface-enhanced resonance Raman scattering (SERRS) has been reported, suggesting that the enhancement factor can reach up to 10^{14} or 10^{15}, thus making the Raman cross sections comparable to the usual cross sections of fluorescence.[14−16] The SERS technique offers many advantages; for example, it is nondestructive, requires little or no sample preparation to obtain structural information, and further allows flexibility in performing measurements in air, vacuum, or solution media.[17−20] Thus, since its discovery in the late 1970s, SERS has been a subject of great interest in many areas of science and technology, including chemical analyses.[21,22] One drawback of SERS is that the enhancement properties of a SERS-active surface are highly dependent on its method of preparation and thus on its detailed nanostructure.[23−25]

On the other hand, a dramatic increase in the fluorescence emission can occur with a nanostructured Ag or Au surface. The phenomenon, called the surface-enhanced fluorescence (SEF) or metal-enhanced fluorescence (MEF), derives from the

Received: July 22, 2012
Accepted: September 27, 2012
Published: October 9, 2012

interaction of the dipole moment of the fluorophore and the surface plasmon field of the metal, resulting in an increase in the radiative decay rate and stronger fluorescence emission.[26,27] In effect, within an optimal range of distances separating molecules from metal, weakly emitting materials (dyes, proteins, or DNA) with low quantum yields can be transformed into more efficient fluorophores with a shortening of fluorescence lifetimes as well. The reduction in fluorescence lifetimes due to MEF means that molecules spend less time in the excited state, thus reducing photobleaching effects.[28] These characteristics of the MEF effect therefore can be utilized in the development of efficient fluorescence-based sensors and microarrays.[28−30]

It was recently discovered that polyethylenimine (PEI) can simultaneously function as a reducing and stabilizing agent to form amine-functionalized Au and Ag nanoparticles.[31,32] The PEI-capped Au and Ag nanoparticles prepared in an aqueous phase could be assembled into 2D arrays not only at the aqueous/toluene interface but also at the inner surface of the sampling bottle simply by the addition of benzenethiol (BT). A Au(Ag) nanoparticle film could be separately formed through brief contact with the mixture on glass slides, inner walls of capillary tubes, or even on dielectric beads and cotton fabrics.[33−35] This Au(Ag)-coated film was highly SERS-active, showing intense peaks of BT. BT could be replaced with other adsorbates by a place-exchange reaction, or more beneficially, it could be removed from the surface of Au(Ag) while maintaining the initial SERS activity by treating with a borohydride solution. PEI is a cationic polyelectrolyte; hence, the properties of Au or Ag films are similar to a positively charged membrane. Nonetheless, the actual surface charge density can vary depending upon the pH of the solution in contact with the film. Another merit of the PEI-capped Au or Ag nanoparticle film is that the surface charges can be further modified with anionic and cationic polyelectrolytes by the layer-by-layer (LbL) deposition technique.[36,37] During LbL deposition, a suitable substrate is dipped back and forth between dilute solutions of positively and negatively charged polyelectrolytes which can also be modified to introduce a wide variety of functional groups. The LbL approach can therefore provide a route to tailor the surface characteristics of nanoparticles and can be used to produce SERS substrates with potential applications such as sensors for biological molecules.[38−40]

In view of the above findings, we examined the characteristics of PEI-capped Ag films and attempted to improve the selectivity of SERS substrates for the detection of charged drug molecules. This report evaluates the SERS and MEF detection of charged dyes, i.e., sulforhodamine B (SRB) and rhodamine-123 (R123), by first using a PEI-capped Ag film and thereafter upon depositing either a strong polyelectrolyte such as poly(sodium 4-styrenesulfonate) (PSS) or a weak polyelectrolyte such as poly(acrylic acid) (PAA) onto the PEI-capped Ag film. Clearly, depending on the assembly conditions employed, either the Raman signal intensity or the fluorescence background became distinct, suggesting that the adopted protocol could enable the design of optimum SERS/MEF substrates to detect charged drug molecules more efficiently.

2. EXPERIMENTAL PROCEDURES

Chemicals. Silver nitrate ($AgNO_3$, 99.8%), sodium borohydride ($NaBH_4$, 99%), BT (>99%), SRB (75%), R123 (85%), branched PEI (MW ∼ 25 kDa), PSS (MW ∼ 70 kDa), PAA (MW ∼ 450 kDa), and silver foil (0.025 mm thickness, 99.9%) were purchased from Aldrich and used as received. Other chemicals unless specified were of reagent grade, and highly purified water with a resistivity >18.0 MΩ·cm (Millipore Milli-Q System) was used for preparing aqueous solutions.

Preparation of PEI-Capped Ag Film. The PEI-stabilized Ag nanoparticles were prepared by boiling a mixture of 100 mL of 10 mM $AgNO_3$ and 1 mL of 2% (w/w) PEI for 15 min. The reacted mixture was centrifuged and decanted, and the precipitate was washed with copious amounts of deionized water.[32] As determined by transmission electron microscopy (TEM) analysis, the average size of the Ag nanoparticles was 14 ± 6 nm (see Figure S1(a) of the Supporting Information). The PEI-stabilized Ag nanoparticles were redispersed in water (5 mL), and toluene (2 mL) was subsequently poured over the aqueous Ag sol. A fairly homogeneous film was formed at the toluene−water interface by adding 1 mL of BT into the toluene phase. A large 2D film was also formed on a separate glass substrate immersed in the mixture (see Figure S1(b) of the Supporting Information), showing an intense UV−vis absorption band at ∼650 nm. For depositing Ag on the inner walls of a capillary (1.1 mm inner diameter × 0.2 mm thickness × 75 mm length), the mixture was injected using a syringe through the capillary tube. BT was desorbed from the PEI-capped Ag nanoparticles without disturbing the SERS activity of the Ag film, by adding a 0.1 M borohydride solution.[34] After the complete disappearance of the SERS peaks of BT, the PEI-capped Ag film was washed with copious amounts of ethanol and then dried with nitrogen.

Instrumentation. The rate of flow through capillary tubes was controlled using a Sage Instruments model 341 syringe pump. UV−vis spectra were obtained with a SINCO S-4100 UV−vis absorption spectrometer. TEM images were taken on a JEM-200CX transmission electron microscope at 200 kV. Field emission scanning electron microscopy (FE-SEM) images were obtained with a JSM-6700F field emission scanning electron microscope operating at 5.0 kV. The zeta potential (ζ) was measured in water by using an electrophoretic light scattering spectrophotometer (ELSZ-1000, OTSUKA Electronics Co. Ltd., Japan): polystyrene (PS, 0.4 μm sized) beads were modified consecutively with PEI-capped Ag nanoparticles and PSS or PAA for this measurement. A quartz crystal microbalance (QCM) experiment was conducted using a Au-coated, AT-cut quartz crystal (fundamental resonance frequency, f_o = 10 MHz): the apparent area of the electrode was 0.20 cm^2. Raman spectra were obtained using a Renishaw Raman system model 2000 spectrometer. The 514 nm line from a 20 mW Ar^+ laser (Melles−Griot model 351MA520) or the 632.8 nm line from a 17 mW He/Ne laser (Spectra Physics model 127) was used as the excitation source. Raman scattering was detected over 180° with a Peltier-cooled (−70 °C) charge-coupled device (CCD) camera (400 × 600 pixels). The data acquisition time was usually 30 s, and the measured intensity was normalized with respect to that of a silicon wafer at 520 cm^{-1}.

3. RESULTS AND DISCUSSION

SRB (Figure 1(a)) is a negatively charged dye.[41] Figure 1(b) shows the UV−vis absorption spectrum of its aqueous 10^{-5} M solution; the absorbance occurred mainly between 460 and 610 nm, and the absorption maximum was observed at 563 nm. Figures 1(c) and (d) show the normal Raman (NR) spectra of aqueous 10^{-5} and 0.1 M solutions of SRB obtained using 514.5 and 632.8 nm as the excitation sources, respectively. As

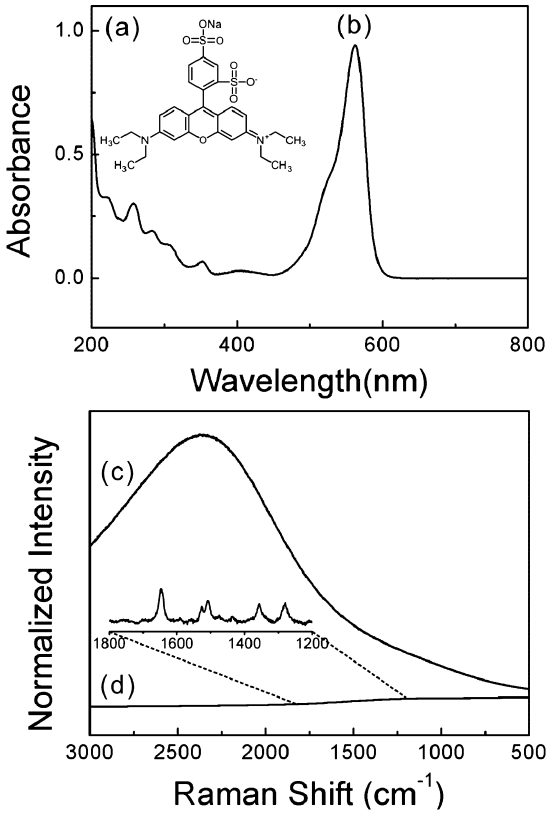

Figure 1. (a) Structure of SRB. (b) UV–vis absorption spectrum of 10^{-5} M aqueous solution of SRB. NR spectra of (c) 10^{-5} M and (d) 0.1 M aqueous solution of SRB measured using 514.5 and 632.8 nm excitation sources, respectively. The inset in (d) shows the magnified spectrum in the 1800–1200 cm^{-1} region.

expected from the UV–vis absorption spectrum, only a strong fluorescence background was seen in the NR spectrum obtained using a 514.5 nm radiation (10^{-5} M of SRB): no peak was identifiable even in an expanded spectrum. In the NR spectrum recorded at 632.8 nm, however, a few bands were identifiable at least on using a concentrated solution (0.1 M of SRB). The bands at 1646, 1528, 1508, 1358, and 1282 cm^{-1} shown in Figure 1(d) (inset) are the characteristic features of xanthene dyes.

Subsequently, SERS activity of the PEI-capped Ag nanoparticle film was initially evaluated by comparing with a HNO_3-etched Ag foil. The Ag foil that was etched with concentrated HNO_3 for 15 s exhibited a strong SERS activity. The SERS signal of BT on a PEI-capped Ag film was 5-fold more intense than that on a HNO_3-etched Ag foil (data not shown), indicating the usefulness of the PEI-capped Ag film as a SERS substrate. As shown in Figure 2(a), on recording the SERS spectrum of HNO_3-etched Ag foil under the flow of 10^{-5} M solution of SRB at a 514.5 nm excitation source, it was difficult to observe the characteristic peaks of SRB. A similar spectrum of PEI-capped Ag nanoparticles (Figure 2(b)) coated on a glass capillary, through which a stream of 10^{-5} M SRB was passed, showed the characteristic peaks of SRB. This was as expected considering that SRB would be present mostly as an anionic species and PEI would be in a protonated state, thus forming an ion pair at pH 7, the pH of a 10^{-5} M solution of SRB. A zeta potential measurement indicates that the PEI-capped Ag nanoparticles are positively charged up to +10.2 mV. On the other hand, it was noted from the open-circuit potential

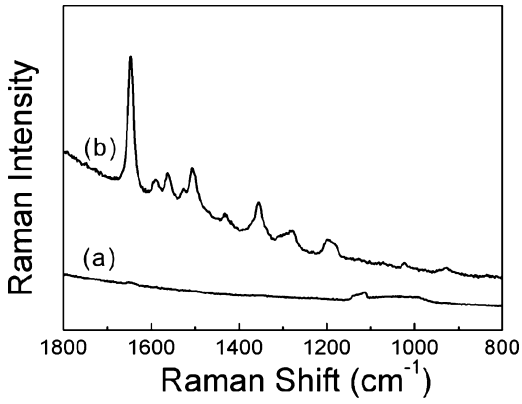

Figure 2. SERS spectrum of 10^{-5} M aqueous solution SRB measured using (a) a HNO_3-etched Ag foil and (b) a PEI-capped Ag nanoparticle film as the SERS substrate: a 514.5 nm excitation source was used.

measurement that the surface of the HNO_3-etched Ag foil was negatively charged; hence, it repelled SRB, resulting in a failure to generate a Raman signal.[42]

Previously, Tan et al. reported that positively charged Ag nanoparticles could be used as an ultrasensitive SERS substrate for in situ measurements of ClO_4^-, SCN^-, CN^-, and SO_4^{2-} in water.[43] Positively charged Ag nanoparticles were first produced by UV-assisted reduction of $AgNO_3$ by using branched PEI and 4-(2-hydroxyethyl)-1-piperazineethanesulfonic acid (HEPES) solutions as reducing agents, and then, they were slowly poured into a glass cell for use as SERS substrates. The detection limit of SCN^-, for instance, was reported to be as low as 1.7×10^{-8} M (1 ppb); such ultrahigh sensitivity was possible because of the synergistic effect of the primary amino groups, which facilitated electrostatic attraction of anions, and the amide groups, which promoted anion attraction by hydrogen bonding and dispersion interactions, formed by the UV irradiation of PEI. Similar work using charged Au nanoparticles to relate SERS to electrostatic field force was reported by Sarkar et al.[44] For comparison, the detection limit of our PEI-capped Ag film was measured for SCN^-, and it was estimated to be as low as 1.0×10^{-9} M (see Figure S2 of the Supporting Information). This value is of the order of a magnitude lower than that reported previously. The PEI-capped Ag film consisted of aggregated Ag nanoparticles; hence, its SERS activity must be greater than that of Ag nanoparticles simply piled onto a solid substrate. The PEIs in the film must also contain amino and amide groups, owing to their reductive action, to produce Ag nanoparticles. It has been previously established that anionic polyelectrolytes such as PAA could be easily deposited, by an LbL method, onto the PEI-capped Ag film, indicating that the surface charge of the Ag film should be highly positive.

The net cationic charge of PEI, as well as the net anionic charge of SRB, depends on the pH of the solution.[36,45] On lowering the solution pH, the net cationic charge of PEI increases, whereas the net anionic charge of SRB decreases. The electrostatic attraction between PEI and SRB is thus dependent on the pH of the solution. Figure 3(a) shows a series of Raman spectra recorded in a stream of 10^{-7} M aqueous solution of SRB at varying pH from 1 to 10 through a glass capillary coated with PEI-capped Ag nanoparticles. All the spectra were obtained using 514.5 nm as the excitation source. In this measurement, the pH was adjusted using either HCl or NaOH.

dx.doi.org/10.1021/am3014168 | ACS Appl. Mater. Interfaces 2012, 4, 5498–5504

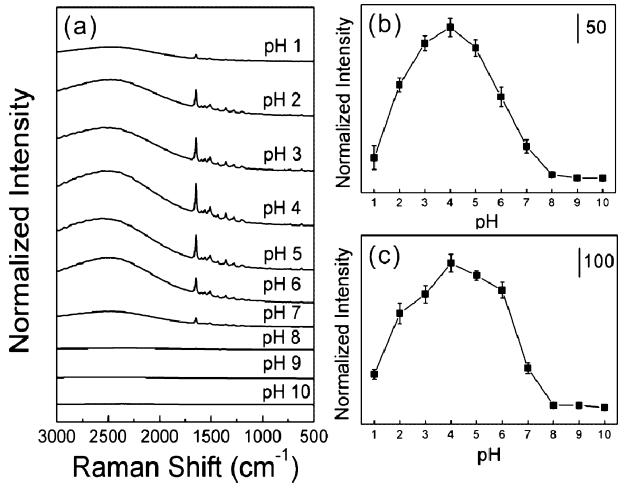

Figure 3. (a) Series of SERS spectra obtained under the flow of 10^{-7} M aqueous solution of SRB at varying pH from 1 to 10 through a PEI-capped Ag capillary tube. The flow rate was 0.19 mL/min. (b) The peak intensity of the xanthene ring mode at 1650 cm^{-1} plotted against the pH of the solution in (a). (c) Intensity of the background fluorescence at 2500 cm^{-1} in (a) plotted against the pH of the solution. For (b) and (c), the error bars indicate the average and standard deviation of 10 different measurements.

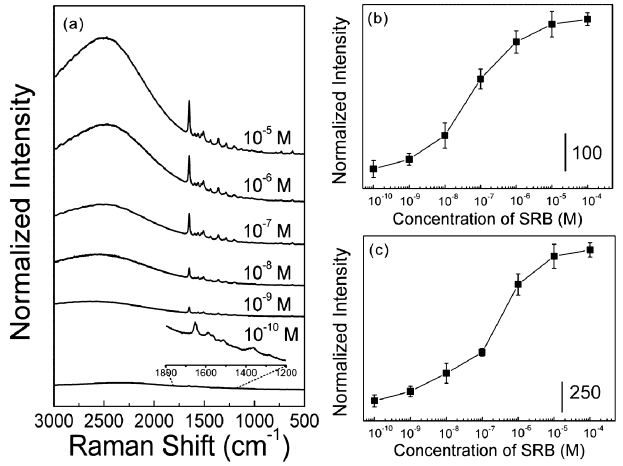

Figure 4. (a) Series of Raman spectra obtained under the flow of $10^{-5} \sim 10^{-10}$ M aqueous solutions of SRB at pH 4 through a glass capillary coated with PEI-capped Ag nanoparticles. All spectra were obtained using a 514.5 nm radiation as the excitation source. The inset shows the expanded spectrum obtained at 10^{-10} M of SRB. (b) The peak intensity of the xanthene ring mode at 1650 cm^{-1} in (a) plotted against the SRB concentration. (c) The intensity of the background fluorescence at 2500 cm^{-1} in (a) plotted against the SRB concentration. For (b) and (c), the error bars indicate the average and standard deviation of 10 different measurements.

As observed from Figure 3(b), the band intensity of the xanthene rings mode at ~1650 cm^{-1} is plotted against the solution pH, and the most intense Raman spectrum was seen at approximately pH 4. This finding implies that at an even lower pH, SRB would be present in a neutral form due to protonation, but at a higher pH, PEI would gradually get neutralized. The infeasible attraction at pH values lower and higher than 4 is also evident from the fluorescence backgrounds in Figure 3(a). SRB is not in contact with Ag but forms an ion pair with PEI; hence, the fluorescence signal of SRB can be enhanced by increasing the interaction with the PEI-capped Ag nanoparticles. As shown in Figure 3(c), a graph of the background fluorescence intensity (recorded at 2500 cm^{-1}) versus the pH of the solution shows the strongest fluorescence at pH 4; this finding is consistent with the Raman signal data.

Subsequently, we examined the efficacy of detection of the Raman signal of SRB using the PEI-capped Ag nanoparticle film. Figure 4(a) displays a series of Raman spectra measured under the flow of $10^{-10} \sim 10^{-5}$ M aqueous solutions of SRB through a glass capillary coated with PEI-capped Ag nanoparticles at pH 4. Again, all the spectra were obtained using a 514.5 nm radiation as the excitation source. The band intensity of the xanthene ring mode at ~1650 cm^{-1} versus the concentration of SRB is illustrated in Figure 4(b). On the other hand, Figure 4(c) shows the intensity of the background fluorescence from Figure 4(a) versus the concentration of SRB. The normalized Raman intensity, as well as the fluorescence intensity, shows a sigmoidal change with the logarithm of the SRB concentration, corresponding to a Frumkin adsorption isotherm.[46,47] The Raman signal of SRB at 10^{-10} M is more than 3-fold greater than the noise level (see the expanded inset of Figure 4(a)), indicating a high probability of detecting subnanomolar concentrations of SRB by Raman spectroscopy using the PEI-capped Ag nanoparticle film as the SERS substrate.

For their normal lifespan, most cells need moderately narrow limits of pH around 7. The interaction of drugs with model membranes at neutral pH will then be worth studying. As noted above, the ion-pair formation of PEI with SRB is less likely at pH 7 than that at pH 4. This is evident from a series of Raman spectra (Figure 5(a)) measured under the flow of $10^{-10} \sim 10^{-5}$ M aqueous solutions of SRB at pH 7 through a glass capillary coated with PEI-capped Ag nanoparticles by using 514.5 nm as the excitation source. Although the peak intensities were reduced in comparison to those obtained at pH 4, as shown in Figure 4(a), the Raman peaks of SRB as well as their background fluorescence were distinguishable at subnanomolar

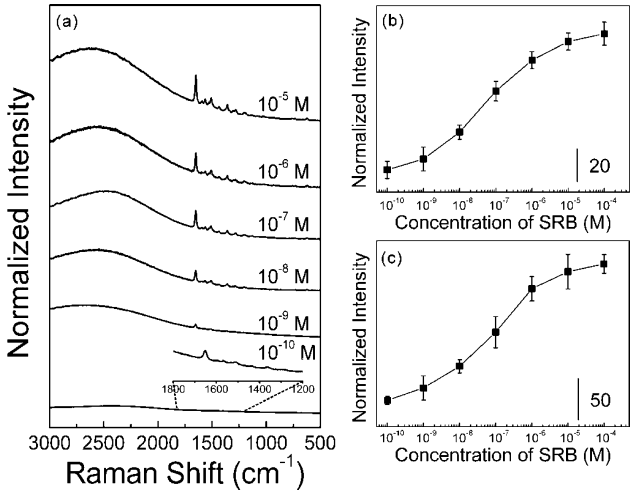

Figure 5. (a) Series of Raman spectra obtained under the flow of $10^{-5} \sim 10^{-10}$ M aqueous solutions of SRB at pH 7 through a glass capillary coated with PEI-capped Ag nanoparticles; all spectra obtained using a 514.5 nm radiation as the excitation source. (b) The peak intensity of the xanthene ring mode at 1650 cm^{-1} and (c) the intensity of the background fluorescence at 2500 cm^{-1} in (a) plotted against the SRB concentration. For (b) and (c), the error bars indicate the average and standard deviation of 10 different measurements.

dx.doi.org/10.1021/am3014168 | ACS Appl. Mater. Interfaces 2012, 4, 5498−5504

concentrations. The Raman intensity and the background fluorescence plotted against the logarithm of SRB concentration are shown in Figures 5(b) and (c), respectively. Although the absolute values in the ordinates are smaller than those in Figures 4(b) and (c), sigmoidal variations were again observed, and the detection limit of SRB at pH 7 appears comparable to that at pH 4, illustrating the usefulness of the PEI-capped Ag nanoparticle film in the detection of anionic drugs by SERS.

It is difficult to detect the presence of cationic drugs by using PEI-capped Ag nanoparticles: in this work, we assumed R123 as a model cationic drug. Its structure and UV−vis absorption spectrum of 10^{-5} M aqueous solution are shown in Figures 6(a) and (b), respectively. The absorption occurred mainly between 420 and 550 nm, with the absorption maximum observed at 500 nm. The NR spectra of 10^{-5} and 0.1 M aqueous solutions of R123 obtained using 514.5 and 632.8 nm radiations as the excitation sources, respectively, are shown in Figures S3(a) and (b) of the Supporting Information. As anticipated from the UV−vis absorption spectrum, only strong background fluorescence was observed in the NR spectrum by using a 514.5 nm excitation source (10^{-5} M of R123); however, several peaks were seen in the NR spectrum obtained at 632.8 nm, especially for a concentrated solution (0.1 M of R123). As mentioned earlier, the peaks at 1643, 1568, 1505, 1369, and 1187 cm^{-1} in the inset of Figure S3(b) of the Supporting Information are characteristic of xanthene dyes,[48,49] and the HNO_3-etched Ag foil attracted R123 because of its negative charge. This finding was confirmed from the Raman spectrum (Figure 6(c)) of a soaking Ag foil in 10^{-5} M aqueous solution of R123 obtained using a 514.5 nm source. No distinguishable peak was detected, as expected, when R123 solution was passed through a glass capillary coated with PEI-capped Ag nanoparticles (data not shown).

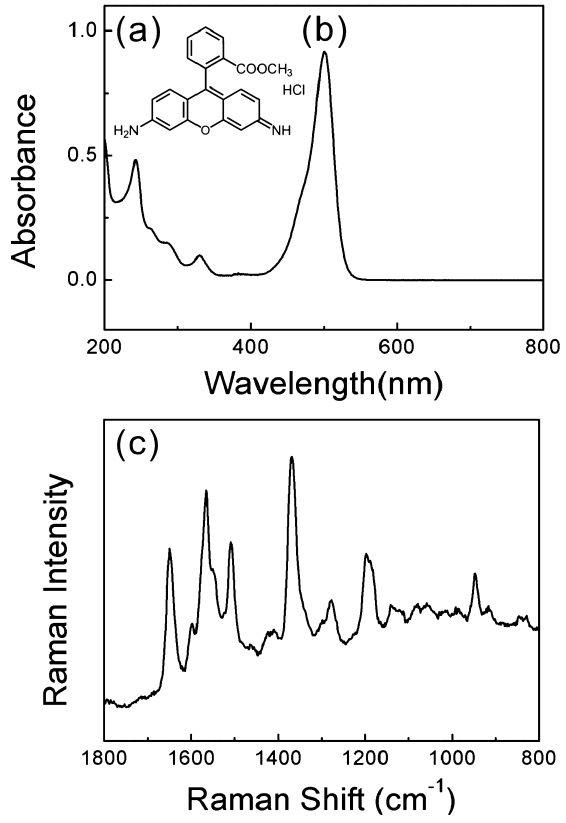

Figure 6. (a) Structure of R123. (b) UV−vis absorption spectrum of 10^{-5} M aqueous solution of R123. (c) SERS spectrum of aqueous 10^{-5} M solution of R123 measured during the flow over a HNO_3-etched Ag foil; a 514.5 nm radiation was used as the excitation source.

To identify R123 by using a PEI-capped Ag nanoparticle film, it is necessary to deposit an anionic polyelectrolyte onto PEI. In the case of Ag nanoparticles that are highly SERS active, the adsorption of R123 even onto the anionic polyelectrolyte would be detectible because of electromagnetic enhancement. Furthermore, the fluorescence signal of R123 was expected to increase markedly with an increase in the gap between Ag and R123 up to some distance. Two different anionic polyelectrolytes were used in this work: PAA, a weak polyelectrolyte, and PSS, a strong polyelectrolyte.[50] A 10^{-3} M aqueous solution of PAA or PSS was injected into a glass capillary previously coated with PEI-capped Ag nanoparticles, and it was allowed to stand for 30 min before blowing out the remaining solution. The glass capillary thus contained either PAA/PEI- or PSS/PEI-capped Ag nanoparticles. However, the net cationic charge of R123 as well as the net anionic charge of PAA/PEI or PSS/PEI were dependent on the pH of the solution. Considering the importance of neutral pH in living systems, we measured the Raman spectra mainly at pH 7 under a flowing solution of R123 through a glass capillary coated with PAA/PEI- or PSS/PEI-capped Ag nanoparticles: The zeta potentials of PSS/PEI- and PAA/PEI-capped Ag nanoparticles at neutral pH were measured to be −35.4 and −17.6 mV, respectively. To estimate the amount of R123 dyes being adsorbed onto the anionic polyelectrolyte-coated Ag nanoparticles, a QCM experiment was conducted. A polyelectrolyte (PSS or PAA)-coated Au electrode was fixed onto a crystal holder using a conductive adhesive, and the holder was fastened onto the QCM cell through the Kalez O-rings. Pure water was first added into the QCM cell and left to stabilize, after which 10^{-7} M aqueous solution of R123 was injected into the cell, monitoring the frequency change as a function of time. As shown in Figure S4 of the Supporting Information, the QCM frequency decreased abruptly by as much as 2−15 Hz. According to the Sauerbrey equation ($\Delta m = -0.884\Delta f$ ng/Hz),[51] the measured frequency change (Δf) corresponded to the adsorption of 1.32×10^{-8} and 1.77×10^{-9} g (Δm) of R123 onto the surfaces of PSS and PAA, respectively. Considering the apparent area of the QCM electrode, the number of R123 molecules bound per 1 μm^2 of PSS and PAA will then be 1.05×10^6 and 1.40×10^5, respectively. Consulting the data in Figure 7(d), those numbers of R123 molecules can readily be identified by SERS.

The Raman spectra measured as a function of R123 concentration ($10^{-10} \sim 10^{-5}$ M) by using a capillary coated with PAA/PEI-capped Ag nanoparticles is shown in Figure 7(a). A 514.5 nm radiation was used as the excitation source; hence, the Raman spectra must be SERRS spectra because of which the Raman peaks could be identified even at subnanomolar concentrations, even though most R123 molecules may be far from the Ag nanoparticles. The normalized Raman intensity of the xanthene mode at ~1650 cm^{-1} plotted against the R123 concentration is displayed in Figure 7(b). Here as well, sigmoidal variation was obtained, indicating a Frumkin-type adsorption isotherm. A similar result could be obtained using a capillary coated with PSS/PEI-capped Ag nanoparticles (Figure 7(c)) for Raman spectra measured using a PSS/PEI-capped Ag nanoparticle film. The Raman signal in Figure 7(c) is of the order of a magnitude

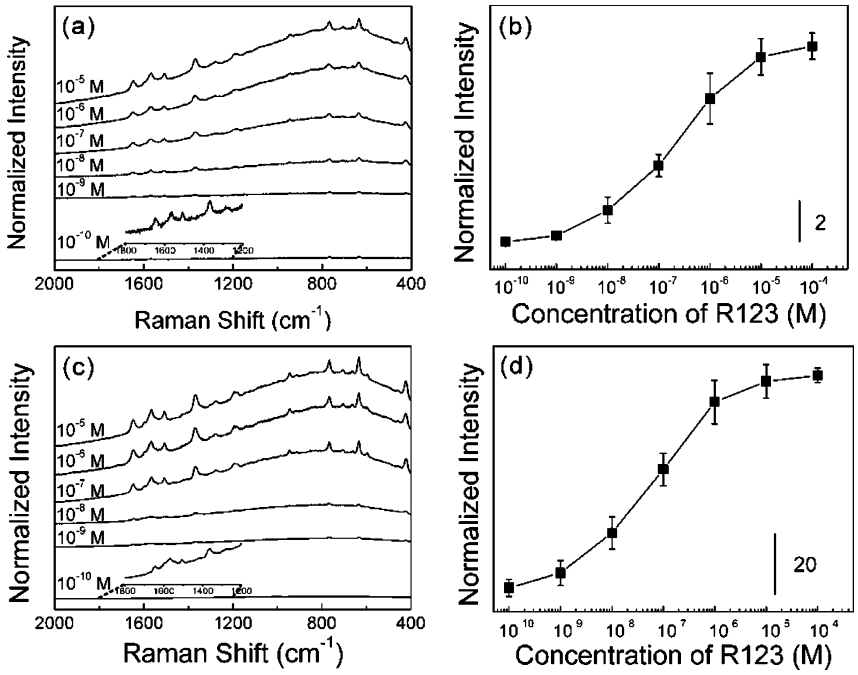

Figure 7. Series of Raman spectra obtained under the flow of $10^{-5} \sim 10^{-10}$ M aqueous solutions of R123 at pH 7 through a glass capillary coated with (a) PAA/PEI- and (c) PSS/PEI-capped Ag nanoparticles. All spectra were obtained using a 514.5 nm radiation as the excitation source. (b) The peak intensity of the xanthene ring mode at 1650 cm^{-1} in (a) and (d) that in (c), drawn against the R123 concentration. For (b) and (d), the error bars indicate the average and standard deviation of 10 different measurements.

stronger than that in Figure 7(a), which could be explained by presuming that the net anionic charge of the PSS/PEI-capped Ag film would be larger than that of the PAA/PEI-capped Ag film. This may be attributed to the strong polyelectrolyte nature of PSS. A more intense Raman signal is more evident from Figure 7(d) in which the xanthene band intensity at ~1650 cm^{-1} is plotted against the R123 concentration. The interaction of R123 with the anionic polyelectrolytes was also confirmed from the background fluorescence as observed from Figures S5(a) and (b) of the Supporting Information in which the background fluorescence intensities from Figures 7(a) and (c), respectively, are plotted against the concentration of R123. Thus, undoubtedly, cationic drug molecules can also be detected by Raman spectroscopy using a PEI-capped Ag nanoparticle film as the SERS substrate.

4. CONCLUSIONS

PEI can function simultaneously as a reducing and stabilizing agent to form amine-functionalized Ag nanoparticles, which can further be fabricated into a 2D film not only onto a glass slide but also onto the inner surface of a glass capillary. It is known that PEI is a cationic polyelectrolyte; therefore, we attempted to demonstrate the usefulness of the PEI-capped Ag nanoparticle film, especially in detecting charged dye molecules by SERS and MEF phenomena. In this light, 14 nm sized, PEI-capped Ag nanoparticles were first produced in an aqueous solution and further fabricated into a PEI-capped, aggregated 2D film. The SERS activity of the PEI-capped Ag nanoparticle film, tested using a prototype organic thiol such as BT, was 5-fold greater than that of a HNO_3-etched Ag foil, and it was possible to detect small-sized anions such as SCN^- at 1×10^{-9} M by SERS, suggesting that the PEI-capped Ag film is useful at least in the detection of anionic dye molecules. In fact, we were able to detect a prototype anionic dye molecule, SRB, not only by SERS but also by MEF at subnanomolar concentrations. pH 4 was optimum for detecting SRB, but a subnanomolar detection limit was achieved even at pH 7. On the other hand, it was difficult to detect cationic dyes such as R123 because of the positive charges of PEI; nonetheless, we found that even R123 could be detected at subnanomolar concentrations not only by SERS but also by MEF, by deposition of an anionic polyelectrolyte such as PSS and PAA onto the PEI-capped Ag nanoparticles. The strong MEF signals observed clearly indicated that SRB and R123 were not in contact with Ag but formed ion pairs with either PEI or PSS (PAA). In line with this finding, the SERS signal of R123 and SRB measured could be associated with the strong electromagnetic enhancement effect of the aggregated Ag nanoparticles. Therefore, the PEI-capped Ag nanoparticle film serves as a useful indicator to detect charged drug molecules by SERS and MEF.

■ ASSOCIATED CONTENT

Ⓢ Supporting Information

TEM and FE-SEM images of PEI-capped Ag nanoparticles, a series of Raman spectra of SCN^- on PEI-capped Ag film, normal Raman spectra of R123, QCM responses of polyelectrolyte-coated Au electrode, and intensity of the background fluorescence. This material is available free of charge via the Internet at http://pubs.acs.org.

■ AUTHOR INFORMATION

Corresponding Author

*Tel.: +82-2-8806651. Fax: +82-2-8891568. E-mail: kwankim@snu.ac.kr (K.K.). Tel.: +82-2-8200436. Fax: +82-2-8244383. E-mail: kshin@ssu.ac.kr (K.S.S.).

Notes

The authors declare no competing financial interest.

■ ACKNOWLEDGMENTS

This work was supported by National Research Foundation (NRF) of Korea grants funded by the Korean Government (MEST) (grants 2007-0056334, 2012-0001352, 2012-0006225, and 2012008004).

■ REFERENCES

(1) Akutsut, H.; Seelig, J. *Biochemistry* **1981**, *20*, 7366−7373.
(2) Beschiaschvili, G.; Seelig, J. *Biochemistry* **1990**, *29*, 52−58.
(3) Barry, J.; Fritz, M.; Brender, J. R.; Smith, P. E. S.; Lee, D. -K.; Ramamoorthy, A. *J. Am. Chem. Soc.* **2009**, *131*, 4490−4498.
(4) Reuter, M.; Schwieger, C.; Meister, A.; Karlsson, G.; Blume, A. *Biophys. Chem.* **2009**, *144*, 27−37.
(5) Sugawara, M.; Takekuma, Y.; Yamada, H.; Kobayashi, M.; Iseki, K.; Miyazaki, K. *J. Pharm. Sci.* **1998**, *87*, 960−966.
(6) Krämer, S. D.; Braun, A.; Jakits-Deiser, C.; Wunderli-Allenspach, H. *Pharm. Res.* **1998**, *15*, 739−744.
(7) Nabiev, I. R.; Morjani, H.; Manfait, M. *Eur. Biophys. J.* **1991**, *19*, 311−316.
(8) Quinn, J. G.; O'Neill, S.; Doyle, A.; McAtamney, C.; Diamond, D.; MacCraith, B. D.; O'Kennedy, R. *Anal. Biochem.* **2000**, *281*, 135−143.
(9) Surewicz, W. K.; Leyko, W. *Biochim. Biophys. Acta* **1981**, *643*, 387−397.
(10) Bagalkot, V.; Zhang, L.; Levy-Nissenbaum, E.; Jon, S.; Kantoff, P. W.; Langer, R.; Farokhzad, O. C. *Nano Lett.* **2007**, *7*, 3065−3070.
(11) Sanganahalli, B. G.; Joshi, P. G.; Joshi, N. B. *Life Sci.* **2000**, *68*, 81−90.
(12) Bacia, K.; Kim, S. A.; Schwille, P. *Nat. Method* **2006**, *3*, 83−89.
(13) Moskovits, M. *Rev. Mod. Phys.* **1985**, *57*, 783−826.
(14) Chang, R. K.; Furtak, T. E. *Surface Enhanced Raman Scattering*; Plenum Press: New York, 1982.
(15) Kneipp, K.; Wang, Y.; Kneipp, H.; Perelman, L. T.; Itzkan, I.; Dasari, R. R.; Feld, M. S. *Phys. Rev. Lett.* **1997**, *78*, 1667−1670.
(16) Nie, S.; Emory, S. R. *Science* **1997**, *275*, 1102−1106.
(17) Yang, Y.; Li, Z.-Y.; Yamaguchi, K.; Tanemura, M.; Huang, Z.; Jiang, D.; Chen, Y.; Zhou, F.; Nogami, M. *Nanoscale* **2012**, *4*, 2663−2669.
(18) Shanmukh, S.; Jones, L.; Driskell, J.; Zhao, Y.; Dluhy, R.; Tripp, R. A. *Nano Lett.* **2006**, *6*, 2630−2636.
(19) Betz, J. F.; Cheng, Y.; Rubloff, G. W. *Analyst* **2012**, *137*, 826−828.
(20) Kao, P.; Malvadkar, N. A.; Cetinkaya, M.; Wang, H.; Allara, D. L.; Demirel, M. C. *Adv. Mater.* **2008**, *20*, 3562−3565.
(21) Halvorson, R. A.; Vikesland, P. J. *Environ. Sci. Technol.* **2010**, *44*, 7749−7755.
(22) Camden, J. P.; Dieringer, J. A.; Zhao, J.; Van Duyne, R. P. *Acc. Chem. Res.* **2008**, *41*, 1653−1661.
(23) Kerker, M. *Acc. Chem. Res.* **1984**, *17*, 271−277.
(24) Stranahan, S. M.; Titus, E. J.; Willets, K. A. *ACS Nano* **2012**, *6*, 1806−1813.
(25) Lee, S. Y.; Hung, L.; Lang, G. S.; Cornett, J. E.; Mayergoyz, I. D.; Rabin, O. *ACS Nano* **2010**, *4*, 5763−5772.
(26) Campion, A.; Gallo, A. R.; Harris, C. B.; Robota, H. J.; Whitmore, P. M. *Chem. Phys. Lett.* **1980**, *73*, 447−450.
(27) Kümmerlen, J.; Leitner, A.; Brunner, H.; Aussenegg, F. R.; Wokaun, A. *Mol. Phys.* **1993**, *80*, 1031−1076.
(28) Lakowicz, J. R. *Anal. Biochem.* **2001**, *298*, 1−24.
(29) Smith, D. S.; Kostov, Y.; Rao, G. *Sens. Actuators, B: Chem.* **2007**, *127*, 432−440.
(30) Sabanayagam, C. R.; Lakowicz, J. R. *Nucleic Acids Res.* **2007**, *35*, e13.
(31) Kim, K.; Lee, H. B.; Lee, J. W.; Park, H. K.; Shin, K. S. *Langmuir* **2008**, *24*, 7178−7183.
(32) Kim, K.; Lee, H. B.; Lee, J. W.; Shin, K. S. *J. Colloid Interface Sci.* **2010**, *345*, 103−108.
(33) Kim, K.; Lee, J. W.; Lee, H. B.; Shin, K. S. *Langmuir* **2009**, *25*, 9697−9702.
(34) Lee, J. W.; Lee, H. B.; Kim, K.; Shin, K. S. *Anal. Bioanal. Chem.* **2010**, *397*, 557−562.
(35) Lee, J. W.; Kim, K.; Shin, K. S. *Vib. Spectrosc.* **2010**, *53*, 121−125.
(36) Kim, K.; Lee, J. W.; Choi, J. -Y.; Shin, K. S. *Langmuir* **2010**, *26*, 19163−19169.
(37) Kim, K.; Lee, J. W.; Shin, D.; Kim, K. Y.; Shin, K. S. *J. Phys. Chem. C* **2010**, *114*, 9917−9922.
(38) Ariga, K.; Ji, Q.; Hill, J. P.; Bando, Y.; Aono, M. *NPG Asia Mater.* **2012**, *4*, e17.
(39) Costa, E.; Lloyd, M. M.; Chopko, C.; Aguiar-Ricardo, A.; Hammond, P. T. *Langmuir* **2012**, *28*, 10082−10090.
(40) Yeo, S. J.; Kang, H.; Kim, Y. H.; Han, S.; Yoo, P. J. *ACS Appl. Mater. Inter.* **2012**, *4*, 2107−2115.
(41) Dos Santos, D S., Jr.; Aroca, R. F. *Analyst* **2007**, *132*, 450−454.
(42) Pérez, R.; Rupérez, A.; Rodriguez-Castellón, E.; Laserna, J. J. *Surf. Interface Anal.* **2000**, *30*, 592−596.
(43) Tan, S.; Erol, M.; Sukhishvili, S.; Du, H. *Langmuir* **2008**, *24*, 4765−4771.
(44) Sarkar, S.; Pande, S.; Jana, S.; Sinha, A. K.; Pradhan, M.; Basu, M.; Chowdhury, J.; Pal, T. *J. Phys. Chem. C* **2008**, *112*, 17862−17876.
(45) Kasnavia, T.; Sabatini, D. A. *Ground Water* **1999**, *37*, 376−381.
(46) Pemberton, J. E.; Buck, R. P. *Anal. Chem.* **1981**, *53*, 2263−2267.
(47) Ko, H.; Chang, S.; Tsukruk, V. V. *ACS Nano* **2009**, *3*, 181−188.
(48) Sarkar, J.; Chowdhury, J.; Pal, P.; Talapatra, G. B. *Vib. Spectrosc.* **2006**, *41*, 90−96.
(49) Chowdhury, J.; Pal, P.; Ghosh, M.; Misra, T. N. *J. Colloid Interface Sci.* **2001**, *235*, 317−324.
(50) Elzbieciak, M.; Kolasinska, M.; Warszynski, P. *Colloids Surface A* **2008**, *321*, 258−261.
(51) Sauerbrey, G. Z. *Phys.* **1959**, *155*, 206−222.